PHASE SINGULARITIES AND TERMINATION OF SPIRAL WAVE REENTRY

James C. Eason, Natalia A. Trayanova
Department of Biomedical Engineering, Tulane University, New Orleans, USA

Abstract— **In order to elucidate the mechanisms by which a strong shock terminates reentrant wavefronts, we employed phase analysis techniques to study phase singularity dynamics in a finite element model of cardiac tissue. We located postshock phase singularities and traced their movement and survival for sixteen monophasic shocks applied at different times during the rotation of a spiral wave. Our analysis revealed that shocks were more likely to succeed when the number of postshock phase singularities was large. Additionally, phase singularities in regions of the tissue exposed to weak shock-induced electric fields were more likely to survive than those in regions of strong shock-induced fields.**

Keywords— **phase singularity, bidomain, cardiac, fibrillation, defibrillation**

I. Introduction

STRONG electrical shocks applied to the heart can terminate an episode of ventricular fibrillation. Efforts to predict the efficacy of these defibrillation shocks rely on empirical methods since links to the growing volume of experimental and theoretical findings regarding defibrillation mechanisms are difficult to forge. To truly advance defibrillation strategies, one must understand the role of these defibrillation mechanisms in the success or failure of a shock and how they manifest themselves in experimental observations of defibrillation efficacy.

An externally applied electric field is capable of inducing changes in transmembrane potential in the myocardium. The change in transmembrane potential can elicit an action potential, prolong the duration of an existing action potential, or deexcite tissue undergoing an action potential [1]. It is known that strong shocks may also cause electroporation of the cell membrane [2] which effectively blocks action potential propagation in the affected tissue. These interactions between an applied field and myocardial tissue form the basis for the mechanisms of defibrillation.

Modeling studies using the bidomain, or multidimensional cable, model of excitable tissue accurately predict interactions between an applied electric field and cardiac tissue [3]. Bidomain analysis described the patterns of membrane polarization induced by an applied field near by [4] and distant from [5] stimulating electrodes. Regions of opposite membrane polarity induced by the shock away from the electrode are referred to as virtual electrode polarization (VEP).

The interactions of VEP and preshock electrical activity have been studied with optical mapping and computer modeling techniques. Experimental observations reveal that strong VEP can completely reset or override the preshock state of the cell membrane [1]. Computational models involving weaker shocks show that success or failure depends upon both the preshock excitable gap and the VEP induced by the shock [6]. These two factors combine in a complex manner to determine the postshock excitable gap in the tissue and the possible existence of postshock phase singularities. Trayanova concluded that the extent and persistence of the postshock excitable gap surrounding a phase singularity is a predictor of the success or failure of the shock [7]. Defibrillation shocks succeed when they can consume the excitable gap between the head and tail of the wavefront while avoiding the creation of new reentrant pathways around shock induced phase singularities [7].

In this paper, we simulate the postshock electrical activity in a two dimensional bidomain reentry model to determine the success or failure of the shock. We investigate the effects of shock timing on pre- and postshock phase singularities in the myocardial tissue [8] and examine the factors leading to their survival in shocks which fail to terminate reentrant behavior.

II. Methods

A. Bidomain Model

We model the excitable tissue as a two dimensional region lying between two concentric circles with radii 1.125 cm and 0.230 cm. As a reference, a mouse heart has a ventricular surface area of approximately 100 square mm which is about one quarter of the size of our tissue. The tissue is anisotropic with a longitudinal fiber axis in the circumferential direction. The tissue is placed in the center of a square domain that measures 2.475 cm on each side. The small circular region in the center of the tissue and the region between the square and the outer circle are conductive bath. We define two electrodes which are used to shock the reentrant wavefront. The cathode is a circle with radius 0.115 cm in the center of the bath. The anode is a line 0.619 cm long centered along the lower edge of the square. The geometry of this model is shown in Fig. 1.

The volume conductor properties of the excitable tissue are described by the bidomain model [3]. We have described this model previously [9]. Briefly, we use the conductivity values from Clerc [10]; membrane dynamics are described by the Beeler-Reuter-Drouhard-Roberge model [11] modified for defibrillation studies [12].

We use the finite element method to solve the bidomain equations on an unstructured mesh consisting of linear triangular elements [9]. The mesh spacing averages 0.023 cm in the tissue and the inner bath and 0.056 cm in the outer bath. The entire mesh consists of 5645 nodes and 11,112 elements. Time derivatives are solved by a semi-implicit backward Euler method with a time step of 1 μs during the stimulus and 10 μs at all other times.

Report Documentation Page

Report Date	Report Type	Dates Covered (from... to)
25 Oct 2001	N/A	-

Title and Subtitle Phase Singularities and Termination of Spiral Wave Reentry	**Contract Number**
	Grant Number
	Program Element Number
Author(s)	**Project Number**
	Task Number
	Work Unit Number
Performing Organization Name(s) and Address(es) Department of Biomedical Engineering Tulane University New Orleans	**Performing Organization Report Number**
Sponsoring/Monitoring Agency Name(s) and Address(es) US Army Research, Development & Standardization Group (UK) PSC 802 Box 15 FPO AE 09499-1500	**Sponsor/Monitor's Acronym(s)**
	Sponsor/Monitor's Report Number(s)

Distribution/Availability Statement
Approved for public release, distribution unlimited

Supplementary Notes
Papers from 23rd Annual International Conference of the IEEE Engineering in Medicine and Biology Society, October 25-28, 2001, held in Istanbul, Turkey. See also ADM001351 for entire conference on cd-rom.

Abstract

Subject Terms

Report Classification unclassified	**Classification of this page** unclassified
Classification of Abstract unclassified	**Limitation of Abstract** UU

Number of Pages
4

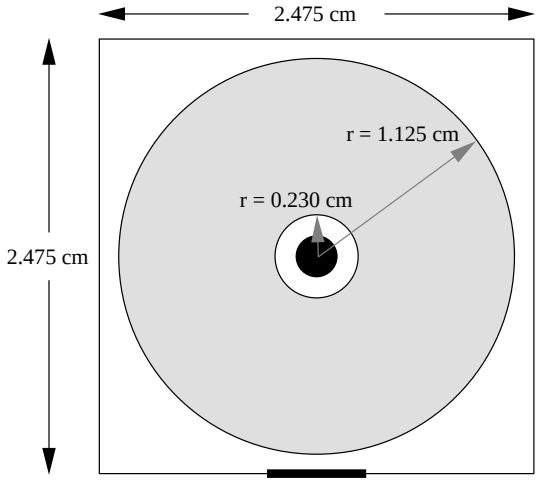

Fig. 1. Geometry of the computational model.

B. Simulation Protocol

A reentry is initiated by eliciting a wavefront moving right to left. A second stimulus is then given to a small region in the lower right hand quadrant of the tissue at a coupling interval of 120 ms. A single spiral wave is created which rotates in a counter-clockwise direction. It completes a single rotation in approximately 80 ms. After two seconds of sustained reentry, we test the ability of a shock to extinguish this spiral.

With a monophasic square waveform of 5 ms duration and a strength of 0.360 A/m, we apply a shock at one of 16 positions of the wavefront shown in Fig. 2. After the shock, the simulation continues for an additional 300 ms. If wavefronts still exist at that time, the shock is considered to have failed; otherwise, it is a success.

III. Results

Membrane polarization induced in tissue at rest by the monophasic shock after 4 ms of the 5 ms duration monophasic stimulus is shown in Fig. 3. In this case, 46% of the tissue has an induced membrane polarization magnitude of 25 mV or greater. The regions occupied by the VEP in this figure will be the ones most affected by the shock in tissue with the reentrant spiral wave.

Shock outcomes were categorized as a success or failure with successes subdivided into type I or type II. Type I is the return of all tissue to rest with no new postshock activations. Type II success is characterized by postshock reentrant activations. In the case of failed shocks, the postshock pattern of reentry consists of either a single phase singularity (a spiral wave), a pair of phase singularities (a figure-of-eight, or two spirals with one shared common pathway), or three phase singularities (three spirals with two shared common pathways). The outcomes of the shocks are summarized in Table I.

Of the successful shocks (7 out of 16), there were an average of 5.7 phase singularities within the tissue at the end of the shock. These persisted for an average of 91 ms after the shock. The type I successes (4 out of 16) had an average

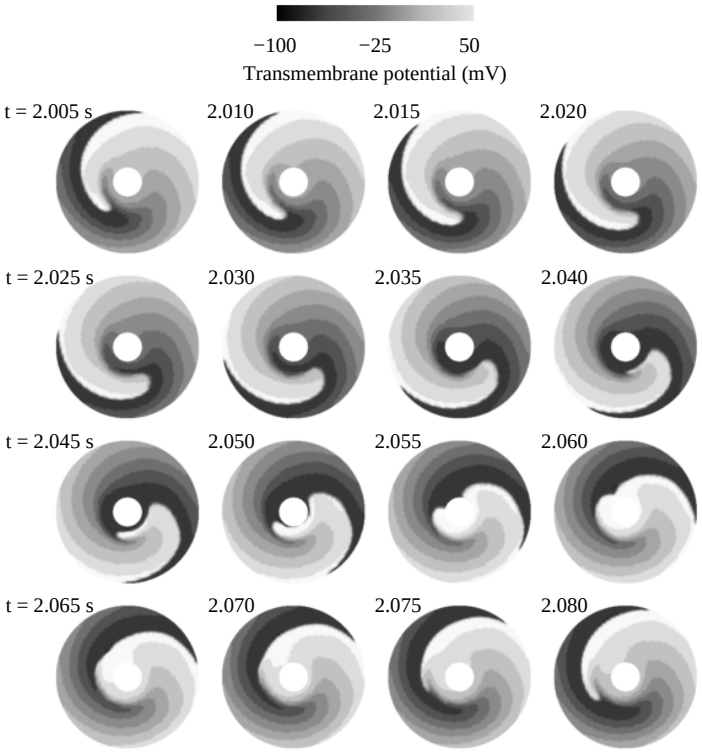

Fig. 2. Wavefront location at each of sixteen discrete times at which a shock is applied to the tissue.

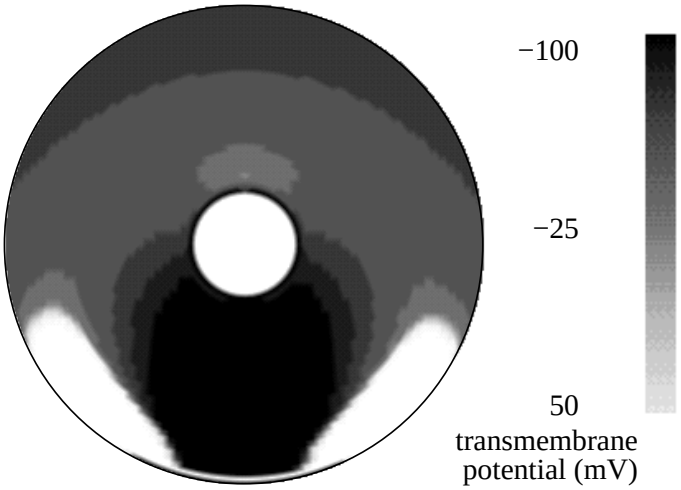

Fig. 3. Transmembrane potential induced by the shock upon tissue initially at rest.

of 5.5 postshock phase singularities which were annihilated within an average of 36 ms (less than one rotation). The type II success (3 out of 16) had an average of 6.0 postshock phase singularities which survived for an average of 164 ms (approximately two rotations). The failed shocks (9 out of 16) had an average of 3.4 postshock phase singularities. One of these cases (shock at 2.015 s) had a total of 7 postshock phase singularities, the remainder of the failed shocks had no more than 4.

Fig. 4 illustrates the dynamics of phase singularity for-

TABLE I
SHOCK OUTCOMES

Time of shock (s)	Outcome	Initial # Phase Sing.	Success Type or Remaining Sing.
2.005	S	7	type II
2.010	S	7	type II
2.015	F	7	2 singularities
2.020	F	4	2 singularities
2.025	S	6	type I
2.030	S	6	type I
2.035	S	6	type I
2.040	S	4	type II
2.045	S	4	type I
2.050	F	2	2 singularities
2.055	F	3	3 singularities
2.060	F	3	3 singularities
2.065	F	3	1 singularities
2.070	F	3	3 singularities
2.075	F	3	2 singularities
2.080	F	3	2 singularities

mation, annihilation, and survival in our myocardial tissue model. In Fig. 4A, phase singularities created by a shock applied at 2.045 s move over time as shown by the tracks on the second panel in Fig. 4A (panel 2, 30 ms after the shock). In this case phase singularities with opposite chirality meet and annihilate one another. No reentry takes place and the shock succeeds.

In Fig. 4B, the shock is applied 5 ms later at 2.050 s, and only two postshock phase singularities are induced in the tissue. These phase singularities move in opposite directions at either end of an activation wavefront which advances quickly towards the tissue cavity. Two additional short-lived phase singularities are created 61 ms after the shock as the wavefront breaks around a region of refractory tissue to the left of the cavity (in panel 2 of Fig. 4B). The two initial phase singularities trace loops along the circumferential fiber direction as a figure-of-eight reentry is established (panel three of Fig. 4B). This new reentrant pattern survives indefinitely and the shock fails.

Finally, we determined the locations of postshock phase singularities in the tissue for each of the 16 shock timings. These locations are shown in Fig. 5. The pattern of phase singularity formation shows that most were formed in the strong potential gradient region between the electrodes. The majority of the phase singularities in this region resulted from successful shocks (i.e., those colored black). Phase singularities created in the low gradient region at the top of the tissue were more likely to survive causing a shock to fail. While this is generally true, there are exceptions. For instance, the shock applied at 2.020 s (denoted by a 3 in Fig. 5) was unsuccessful despite creating postshock phase singularities only in the high gradient region between the electrodes. The shock applied at 2.040 s (denoted by a 7 in Fig. 5) resulted in an equal number of postshock phase singularities in similar locations, however, it was successful.

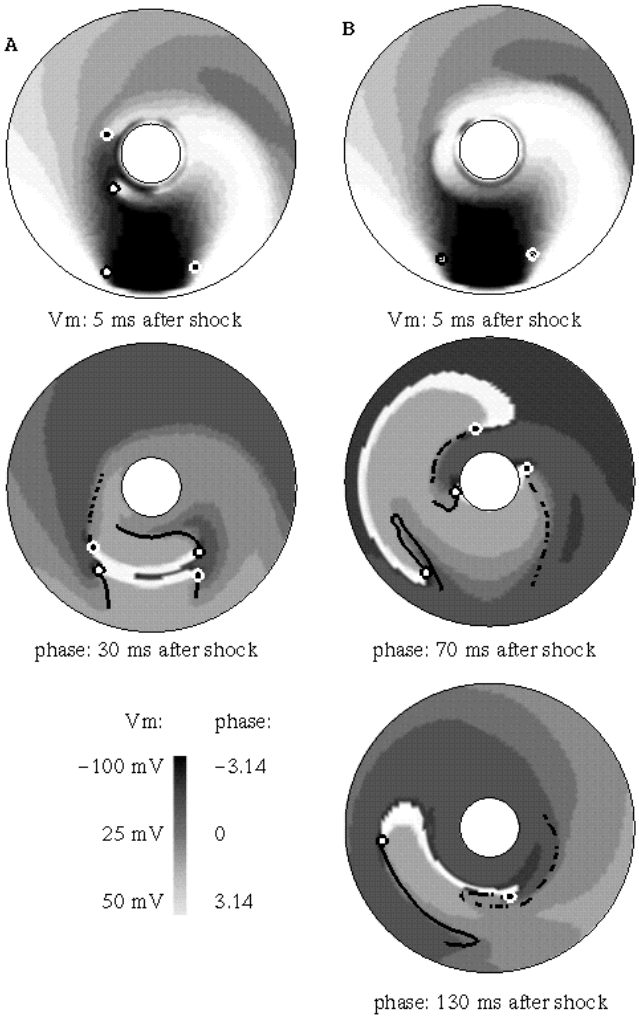

Fig. 4. Phase singularity formation and survival after a strong shock. In each case, the first panel shows transmembrane potential, the following panels show phase, and the locations and tracks of phase singularities are marked with a circle. A white circle with a black center denotes a phase singularity with a counterclockwise rotating activation wavefront, while a black circle with a white center denotes the opposite chirality. (A) A shock is applied at 2.045 s creating four phase singularities which collide and annihilate one another. (B) An ultimately unsuccessful shock is applied at 2.050 s creating two phase singularities. Each of these singularities survives resulting in a figure-of-eight reentry.

IV. DISCUSSION

The analysis techniques described in this study provide a mechanistic insight into the termination of reentry by revealing the dynamics of postshock phase singularity formation and survival in cardiac tissue exposed to an applied field. We show that a strong extracellular field will induce phase singularites in reentrant tissue which then interact to determine the outcome of the shock.

Analysis of our results reveals a surprising trend – shocks are more likely to succeed when they create more postshock phase singularities. A possible explanation for this phenomena may be found in the topological analysis of phase singularities. Once a phase singularity forms in an excitable media, it will survive until it either collides with a singu-

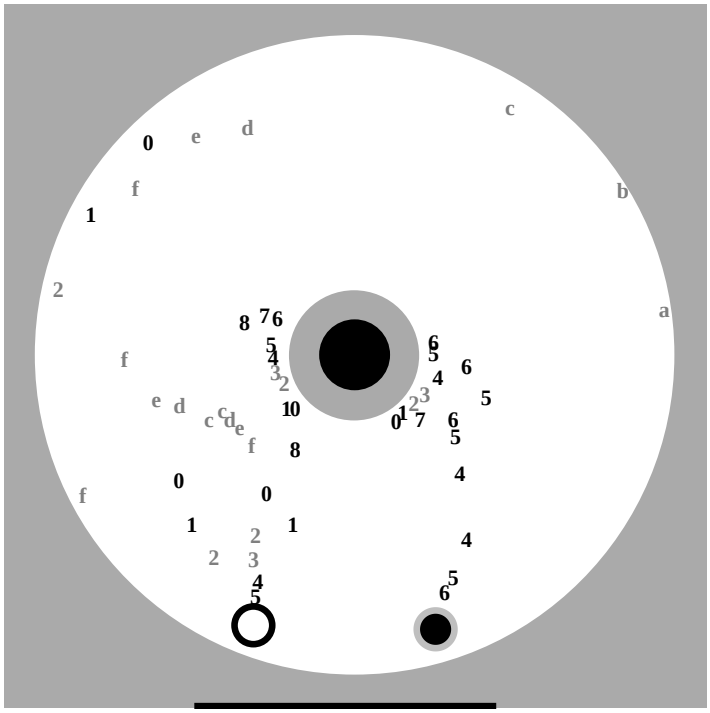

Fig. 5. Location of postshock phase singularities. The location of a phase singularity immediately following a shock is marked by a number or letter corresponding to one of the sixteen shock timings shown in Fig. 2 (consecutively denoted by 0 through 9 and a through f). Characters representing a failed shock are gray while those representing successful shocks are black. The two circles at the bottom of the figure show the locations of the shock induced phase singularities which existed in virtually all of the simulations.

larity of opposite chirality or it wanders across a boundary. When few phase singularities are formed after a shock, it is less likely that all will find an opposing singularity to mutually annihilate. Thus, it is more likely that one or more will survive and sustain reentry in the tissue.

Though this trend is fairly consistent in our results, there are notable exceptions. The shock at 2.015 s failed after creating 7 postshock phase singularities. Also, the shocks at 2.020 s and 2.040 s had different outcomes despite creating a similar set of postshock phase singularities. These exceptions are likely due to the fact that postshock gradients in refractoriness also play a role in determining the survival of individual phase singularities. These gradients in refractoriness can push or pull a phase singularity to follow a particular path as it moves over time. The path, of course, determines whether a phase singularity is likely to collide with a singularity of opposite chirality or a border.

Finally, our results suggest that postshock phase singularities located in low gradient regions (whether they are induced by a shock or remnants from the preshock activity) have a high likelihood of surviving to reinitiate reentry and cause a shock to fail. The locations of the phase singularities in failed shocks denoted by the letters a through f in the upper portion of Fig. 5 are the basis for this conclusion. These phase singularities are located along the tail of the preshock spiral wave. It is obvious that the low impact of the shock in this upper portion of the tissue was not able to prevent the continued propagation and reentry of these spiral waves.

Our results are generally consistent with hypotheses regarding defibrillation mechanisms. Previous experimental [13] and theoretical [7] analyses of defibrillation mechanism describe the importance of limiting the excitable gap around postshock phase singularities. Failure to do so leads to the failure of shocks applied between 2.055 s and 2.080 s in our simulations. However, no analysis of defibrillation mechanisms has suggested that increasing the number of postshock phase singularities may increase the likelihood of successful defibrillation. In fact, efforts have been made to design defibrillation waveforms to minimize the creation of postshock phase singularities. Further research is required to determine if this particular trend in our results will hold true in more complicated defibrillation models and for a variety of shock waveforms and strengths.

V. Acknowledgment

This work was supported by NSF Grants BES-9809132 and DMF-9709754, and NIH Grant HL63195.

References

[1] I. R. Efimov, Y. N. Cheng, D. R. Van Wagoner, T. N. Mazgalev, and P. J. Tchou, "Virtual electrode-induced phase singularity: a basic mechanism of defibrillation failure," *Circulation Research*, vol. 82, pp. 918–25, May 1998.

[2] W. Krassowska, "Effects of electroporation on transmembrane potential induced by defibrillation shocks," *Pacing and Clinical Electrophysiology*, vol. 18, pp. 1644–1660, 1995.

[3] C. S. Henriquez, "Simulating the electrical behavior of cardiac muscle using the bidomain model," *Critical Reviews in Biomedical Engineering*, vol. 21, pp. 1–77, 1993.

[4] J. P. Wikswo Jr, T. A. Wisialowski, W. A. Altemeier, J. R. Balser, H. A. Kopelman, and D. M. Roden, "Virtual cathode effects during stimulation of cardiac muscle," *Circulation Research*, vol. 68, pp. 513–530, 1991.

[5] S. B. Knisley, N. A. Trayanova, and F. Aguel, "Roles of electric field and fiber structure in cardiac electric stimulation," *Biophysical Journal*, vol. 77, pp. 1404–1417, 1999.

[6] K. Skouibine, N. Trayanova, and P. Moore, "Success and failure of the defibrillation shock: insights from a simulation study," *Journal of Cardiovascular Electrophysiology*, vol. 11, pp. 785–796, July 2000.

[7] N. A. Trayanova, "Concepts of defibrillation," *Phil Trans Roy Soc London A*, vol. 359, pp. 1327–1337, 2001.

[8] R. A. Gray, A. Pertsov, and J. Jalife, "Spatial and temporal organization during cardiac fibrillation," *Nature*, vol. 392, pp. 675–678, 1998.

[9] J. C. Eason and R. A. Malkin, "A simulation study evaluating the performance of high-density electrode arrays on myocardial tissue," *IEEE Transactions on Biomedical Engineering*, vol. 47, pp. 893–901, 2000.

[10] L. Clerc, "Directional differences of impulse spread in trabecular muscle from mammalian heart," *Journal of Physiology*, vol. 255, pp. 335–346, 1976.

[11] J.-P. Drouhard and F. A. Roberge, "Revised formulation of the Hodgkin-Huxley representation of the sodium current in cardiac cells," *Comp & Biomed Res*, vol. 20, pp. 333–350, 1987.

[12] K. Skouibine, N. A. Trayanova, and P. K. Moore, "A numerically efficient model for simulation of defibrillation in an active bidomain sheet of myocardium," *Mathematical Biosciences*, vol. 166, pp. 85–100, 2000.

[13] I. R. Efimov, Y. N. Cheng, Y. Yamanouchi, and P. J. Tchou, "Direct evidence of the role of virtual electrode-induced phase singularity in success and failure of defibrillation," *Journal of Cardiovascular Electrophysiology*, vol. 11, no. 8, pp. 861–868, 2000.